AGU PUBLICATIONS

JGR

Journal of Geophysical Research: Biogeosciences

RESEARCH ARTICLE
10.1002/2015JG003065

Key Points:
- Increasing DOC load over the past 30 years lengthened anoxic periods in lake
- Increasing air temperature shortened ice cover and caused enhanced water column ventilation
- The effect of DOC and temperature on DO is compared using a process-based model

Supporting Information:
- Supporting Information S1

Correspondence to:
R.-M. Couture,
rmc@niva.no

Citation:
Couture, R.-M., H. A. de Wit, K. Tominaga, P. Kiuru, and I. Markelov (2015), Oxygen dynamics in a boreal lake responds to long-term changes in climate, ice phenology, and DOC inputs, *J. Geophys. Res. Biogeosci.*, *120*, 2441–2456, doi:10.1002/2015JG003065.

Received 25 MAY 2015
Accepted 27 OCT 2015
Accepted article online 3 NOV 2015
Published online 25 NOV 2015

Oxygen dynamics in a boreal lake responds to long-term changes in climate, ice phenology, and DOC inputs

Raoul-Marie Couture[1,2], Heleen A. de Wit[1], Koji Tominaga[1,3], Petri Kiuru[4], and Igor Markelov[2]

[1]Norwegian Institute for Water Research, Oslo, Norway, [2]Department of Earth and Environmental Sciences, University of Waterloo, Waterloo, Canada, [3]Now at Department of Biosciences, University of Oslo, Oslo, Norway, [4]Freshwater Center, Finnish Environment Institute, Jyväskylä, Finland

Abstract Boreal lakes are impacted by climate change, reduced acid deposition, and changing loads of dissolved organic carbon (DOC) from catchments. We explored, using the process-based lake model MyLake, how changes in these pressures modulate ice phenology and the dissolved oxygen concentrations (DO) of a small boreal humic lake. The model was parametrized against year-round time series of water temperature and DO from a lake buoy. Observed trends in air temperature (+0.045°C yr^{-1}) and DOC concentration (0.11 mg C L^{-1} yr^{-1}, +1% annually) over the past 40 years were used as model forcings. A backcast of ice freezing and breakup dates revealed that ice breakup occurred on average 8 days earlier in 2014 than in 1974. The earlier ice breakup enhanced water column ventilation resulting in higher DO in the spring. Warmer water in late summer led to longer anoxic periods, as microbial DOC turnover increased. A long-term increase in DOC concentrations caused a decline in lake DO, leading to 15% more hypoxic days (<3 mg L^{-1}) and 10% more anoxic days (<15 µg L^{-1}) in 2014 than in 1974. We conclude that climate warming and increasing DOC loads are antagonistic with respect to their effect on DO availability. The model suggests that DOC is a stronger driver of DO consumption than temperature. The browning of lakes may thus cause reductions in the oxythermal habitat of fish and aquatic biota in boreal lakes.

1. Introduction

Dissolved oxygen concentration ($O_{2(aq)}$, hereafter referred to as DO) is a fundamental parameter in aquatic ecosystems [*Wetzel*, 2001] and a priority for freshwater management [*Cooke et al.*, 2005]. The concentration of DO is a critical factor in structuring biological communities both in the sediment and the water column of lakes. In the former, it regulates the biogeochemical processes leading to carbon burial in sediment or degradation during diagenesis [e.g., *Gelda et al.*, 2013; *Kraal et al.*, 2013; *Müller et al.*, 2012; *Palastanga et al.*, 2011], and in the latter it controls fish metabolism [*Dillon et al.*, 2003; *Jiang et al.*, 2012]. Economically, important cold water fish such as salmon and brown trout thrive in an oxythermal habitat which combines high DO concentrations and low water temperatures [*Dillon et al.*, 2003; *Jiang et al.*, 2012], typical for the hypolimnion of natural boreal oligotrophic lakes.

The main biogeochemical processes contributing to variability of DO in a lake are oxygen production during daylight by autotrophs, physical exchange of oxygen between water and the atmosphere, and oxygen consumption by respiring organisms, for which O_2 acts as the terminal electron acceptor [*Staehr et al.*, 2010]. In boreal oligotrophic lakes, respiration is largely controlled by the availability of labile organic matter (OM) as an electron donor [*Bertilsson et al.*, 2013]. DO consumption in the course of OM degradation occurs in the water column and in the sediment, resulting in the release of carbon dioxide, ammonia and phosphate.

The formation of lake ice is another chief factor controlling DO supply to the water column. Ice formation depends on climate drivers, which control the storage of heat within the lake, and on the local weather conditions that control freezing via the net heat exchange between a lake and the atmosphere, wind speed, air temperature, and precipitation [*Livingstone and Adrian*, 2009]. This interplay between climatic drivers and ice formation is captured by empirical [e.g., *Livingstone and Adrian*, 2009] and process-based models for lake ice [e.g., *Saloranta and Andersen*, 2007]. Seasonal ice and snow cover diminish the renewal of water from the catchment, hindering water mixing [*Blenckner et al.*, 2010; *Kirillin et al.*, 2012]. As underwater light penetration and wind-driven atmospheric exchange of O_2 between the atmosphere and the lake's surface decrease, oxygenic

photosynthesis and lake metabolism slow down [*Bertilsson et al*., 2013]. Algal communities may then rely on heterotrophic metabolism for growth [*Salonen et al*., 2009]. Under these conditions, the water column is more physically stable and DO is not replenished from the atmosphere. The rate of DO depletion under ice is then primarily a function of lake volume, the rate of OM diagenesis, and of the allochthonous inputs of dissolved organic carbon (DOC) [*Bertilsson et al*., 2013; *Clilverd et al*., 2009]. The presence of ice cover and its duration (i.e., ice phenology) have thus a profound impact on lake DO dynamics and on the physical and chemical characteristics of the lake [*Golosov et al*., 2012; *Terzhevik et al*., 2010].

Large-scale, long-term changes in climate have impacted lake ice phenology in Nordic lakes [*Arp et al*., 2013; *Kheyrollah Pour et al*., 2012; *Magnuson et al*., 2000; *Weyhenmeyer et al*., 2011]. Changed lake ice dynamics have driven transitions in lake mixing regime [*Livingstone and Adrian*, 2009] and have modified the timing and magnitude of primary productivity [*Blenckner et al*., 2010] through effects on light penetration and wind-induced water column mixing. Despite the usefulness of lake ice as an indicator of climate change, ground-based observational recording has decreased dramatically since the 1980s [*Blunden and Arndt*, 2013]. Satellite remote sensing has since assumed an important role in lake ice monitoring [*Duguay et al*., 2013; *Kheyrollah Pour et al*., 2012], but such studies focus primarily on lakes with at least 1 km^2 continuous, land-free surface area. Thus, lakes with a surface area of <1 km^2, which are abundant globally and represent an estimated 20% of total lake surface area [*Downing et al*., 2006; *Verpoorter et al*., 2014], are neglected. There are few published long-term time series of ice phenology available for Norway, as exemplified by the scarcity of entries in the Global Lake and River Ice Phenology database [*Benson and Magnuson*, 2012]; only Lake Mjøsa—Norway's largest lake—is represented.

In addition to changes in ice phenology, boreal lakes are also impacted by "browning," i.e., have received higher loadings of DOC, as evidenced by water chemistry records for a large number of headwater lakes and lower order streams across northern Europe and North America [*Monteith et al*., 2007; *Skjelkvale et al*., 2007]. Boreal lakes, where browning occurs, are usually small, shallow, oligotrophic, acidic, and in formerly glaciated landscapes with thin soils. Some of these lakes are humic or became so as a result of sustained inputs of DOC originating in the catchments [*Blenckner et al*., 2010], i.e., allochthonous DOC. Although the definition of "humic lake" is arbitrary, the term denotes a category of lakes that has low pH and high-DOC concentrations (e.g., DOC ≥ 10 mg L^{-1}). The DOC is colored and has high aromaticity and a tendency to flocculate [*Kothawala et al*., 2014], and its effects on light absorbance can modify the stratification properties of the water column [*Fee et al*., 1996]. Although the response of lake productivity to higher DOC loads is manifold, recent literature suggests that DOC decreases lake productivity mainly via DOC-driven light attenuation [*Finstad et al*., 2014] and DO consumption [*Craig et al*., 2015].

Small boreal lakes are sensitive to allochthonous DOC loads as a driver of lake metabolism [*Brothers et al*., 2014] and to seasonal ice cover as a limiting factor for DO replenishment [*Kirillin et al*., 2012; *Terzhevik et al*., 2010]. Here we use a process-based lake modeling approach [e.g., *Fang and Stefan*, 2009] to disentangle the respective effects of changing climate and DOC loads on DO, as well as their possible interaction. We update a long-term data set (1973–2003) on hydrology and DOC flux data [*De Wit et al*., 2008, 2007; *Futter and de Wit*, 2008] with the data from the latest decade (2004–2014) and combine it with a new data set on long-term ice phenology (1974–2014) and high-frequency monitoring of water column temperature and DO (2010–2014) in the humic boreal lake Langtjern, in Norway. Lake Langtjern is representative of a large portion of boreal lakes, most of which cover a small area [*Verpoorter et al*., 2014], has a seasonal yet shortening ice cover [*Duguay et al*., 2013], an acidic to circum-neutral water column chemistry [*Garmo et al*., 2014], and high humic content [*Henriksen et al*., 1998]. Using data sets with different temporal resolutions and lengths facilitates differentiation between the two drivers of DO availability, in a decadal and short-term event perspective.

2. Method

2.1. Study Site

The Langtjern catchment (4.8 km^2) is located in southeast Norway (60.372 latitude, 9.727 longitude) at 510 to 750 m elevation approximately 80 km northwest of Oslo (Figure 1). It is undisturbed and comprises predominantly pine forest on thin soils interspersed with peat lands. It has been included in the Norwegian national monitoring program for effects of acid deposition since 1972. Lake Langtjern is acidic, humic, and oligotrophic. The length of the lake is ~1 km, and it consists of three basins, of which the southern basin is the largest and

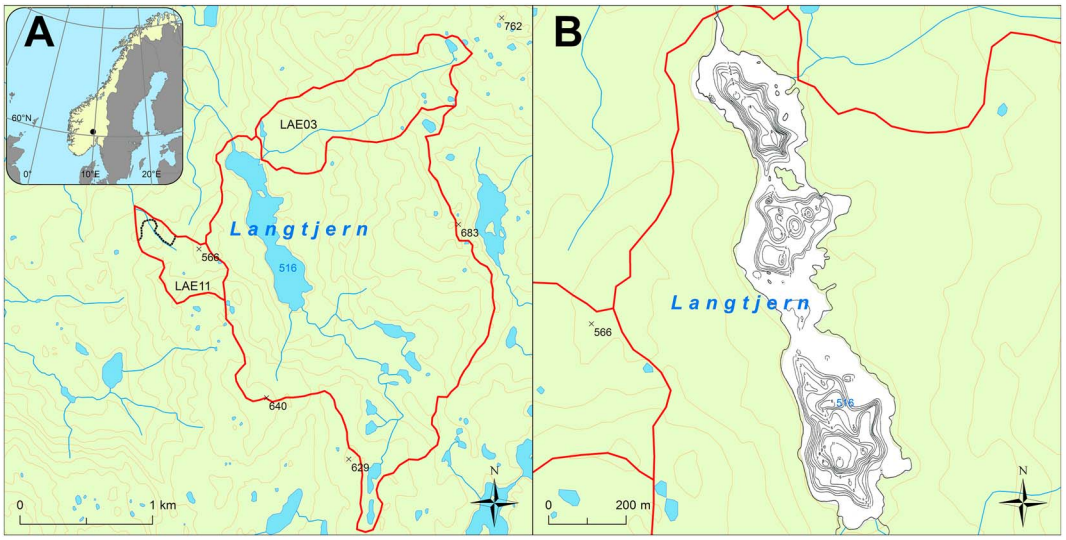

Figure 1. (a) Location of Lake Langtjern and (b) bathymetry of the three basins (B). The solid line denotes the boundary of the catchment and of the main tributaries.

deepest. The lake is fed by two main inlet streams, and the outlet drains the lake toward the north. The characteristics of the lake are given in Table 1.

2.2. Weather Data

A weather station located at the eastern lake shore of the northern basin has measured daily air temperature (T_{Air}) since 2006 and was upgraded in November 2012 for radiation, relative humidity, and wind speed and finally for precipitation in May 2013. Prior to that (1972–2006), weather data were obtained from the meteorological station Gulsvik-II (# 24710; elevation 142 m above sea level (asl); 60.383 latitude, 9.605 longitude) located 6.8 km from Lake Langtjern. T_{Air} at the study site was obtained by correcting the measured T_{Air} at Gulsvik-II by 0.46°C per 100 m and precipitation by correcting by a multiplication factor of 1.17. The adjustments were based on the comparison between the Gulsvik-II station and the on-site weather and runoff station at the lake, since both stations are now running simultaneously for all measured parameters. Coefficient of determination (r^2) between daily T_{Air} measured at Langtjern and those corrected from Gulsvik-II is of 0.99, and of 0.92 for annual discharge. Wind speeds from Gulsvik-II were used uncorrected throughout the simulation. Potential biases between the station Gulsvik-II and the local winds are accounted for when the fraction of turbulent kinetic energy from the wind applied at the lake surface is parametrized using the wind sheltering coefficient in the lake model [*Hondzo and Stefan*, 1993; *Saloranta and Andersen*, 2007].

Table 1. General Characteristics and Chemistry[a] of Lake Langtjern, Norway

Longitude	9.727
Latitude	60.372
Altitude	516 m asl
Lake surface area	0.23 km^2
Catchment area	4.8 km^2
Lake volume	5.6×10^5 m^3
Maximum lake depth	12 m
Thermocline range	1–3 m
Mean lake depth	2 m
Mean outlet discharge[b]	524 mm yr^{-1}
Secchi depth	1.4 m
pH	5.04
Chlorophyll *a*	2.0 μg L^{-1}
DOC	11.3 mg L^{-1}
Alkalinity	0.029 mmol L^{-1}
NO_3^- (as NO_3^-)	11 μg L^{-1}
TN	271 μg L^{-1}
TP	5.2 μg L^{-1}
Fe[c]	0.26 mg L^{-1}
SO_4^{2-}	0.84 mg L^{-1}

[a]Mean of 2010–2013 period, measured at the lake outlet. Source: NIVA.
[b]Mean of 2010–2013 period. Source: Norwegian water resources and energy directorate.
[c]Mean of 2006–2008 period, measured at the lake outlet. Source: NIVA.

2.3. Runoff and Water Chemistry

Discharge was recorded continuously by way of a V notch weir at the outlet of Langtjern, while total discharge to

the lake was estimated based on a full water balance for the entire lake catchment, using precipitation data, estimated evapotranspiration from the lake, changes in lake water storage related to lake level variations, and outlet discharge [*De Wit et al*., 2014]. Temperature of the inflowing streams (T_{Water}) was calculated based on daily T_{Air} [*Stefan and Preud'homme*, 1993]. Biweekly to monthly measurements of water chemistry parameters and total organic carbon concentration (TOC) in the inlets and outlet (Table 1) were performed at the Norwegian Institute for Water Research (NIVA) according to procedures established in the ICP Waters program [*ICP Waters*, 2010]. At our site, TOC is a good proxy for dissolved organic carbon concentration (DOC, defined as the fraction passing through a 0.45 μm filter): parallel measurements of TOC and DOC showed that particulate organic carbon (TOC-DOC) was on average 3% and 4% of TOC in the inlet ($n = 24$, January to November 2007) and outlet ($n = 24$, September 2006 to November 2007 and $n = 39$, January 2011 to December 2012), respectively. The analytical method used and weekly TOC data from 1986 to 2004 is presented in *De Wit et al*. [2007]. Here we extend this data set and present new data from 2004 to 2014.

2.4. Ice

A record of ice phenology observed during site visits was maintained sporadically from 1974 to 2011 and recorded using an on-site time-lapse camera (Figure S1 in the supporting information (SI)) from 2011 to 2014. The record consists of (1) observed breakup days ($n = 10$), (2) intervals within which breakup days is known to have occurred ($n = 10$), (3) observed freezing dates ($n = 18$), and (4) intervals within which freezing is known to have occurred ($n = 9$).

2.5. In-Lake Temperature and DO Sensors

High-frequency sensors were deployed in the lake on a buoy and at the outlet on 27 May 2010. The lake buoy sensors monitor T_{Water} and DO (Oxygen Optode 4330, Aanderaa Instruments) with 2 h and 0.5 h intervals, respectively. These frequencies were chosen in order to allow calculation of heat and DO budgets while minimizing energy consumption of the buoy, which is powered by solar panels. T_{Water} has been monitored at eight depth intervals (0.5, 1, 1.5, 2, 3, 4, 6, and 8 m) and DO at two depth intervals (1 and 8 m) in the northern basin since May 2010. The buoy remains in the lake all winter, providing under-ice measurements. The data are transmitted to NIVA via a GSM service.

2.6. Modeling Approach

Process-based lake models possess several advantages over empirical ones because in-lake phenomena, such as wind-induced physical mixing, heat capacity, and penetration of short-wave radiation, are all dependent on daily stochastic weather progression and need to be explicitly accounted for [*Fang and Stefan*, 2009]. One-dimensional (1-D) process-based models are convenient tools to study lake basins for which the bathymetry and hydrodynamics allow for assumptions of horizontal homogeneity. One-dimensional models are used, for instance, to access the impact of climate on lake thermal regimes [*Dibike et al*., 2012; *Hondzo and Stefan*, 1993; *Read et al*., 2014], ice formation [*Gebre et al*., 2014; *Kheyrollah Pour et al*., 2012; *Rooney and Bornemann*, 2013], DO dynamics [*Fang and Stefan*, 2009; *Golosov et al*., 2012; *Peña et al*., 2010; *Rucinski et al*., 2014], and phytoplankton blooms [*Couture et al*., 2014; *Robson*, 2014; *Trolle et al*., 2011, 2014].

Here we use three-chained setups of the 1-D, process-based daily time step lake model MyLake. MyLake is a MATLAB package designed for the simulation of seasonal ice formation, snow cover, water column stability, daily distribution of heat, phosphorus species dynamics, and phytoplankton abundance in the water column [*Saloranta and Andersen*, 2007]. Light absorption by water, phytoplankton, colored DOC, light scattering, and shading allows calculation of light attenuation. It follows that light availability then limits DOC photobleaching and phytoplankton growth. MyLake uses a stacked layer geometry consisting of mixed horizontal layers. Its hydrodynamic module (1) calculates daytime and nighttime surface heat fluxes and heat sources, turbulent kinetic energy from wind (in the absence of an ice cover), and heat fluxes between water and sediment; (2) performs convective mixing; and (3) applies a routine to calculate the vertical turbulent diffusion coefficient and the settling of solid components. If the density of the inflow is less or equal than the density of the surface layer, the inflow is mixed with the surface layer. Otherwise, the inflow is added on top of the first layer heavier than it, thus lifting an equal amount of outflowing water and conserving lake volume. However, the model does not handle water inflows from groundwater (see section 4.2). The model is forced by time series of daily meteorological input data

comprising global radiation, cloud cover, T_{Air}, relative humidity, air pressure, wind speed and precipitation, inflow volumes, and geochemical fluxes.

MyLake has been applied to several lakes in Norway, Finland, and Canada to simulate lake stratification and ice phenology [*Dibike et al*., 2012; *Gebre et al*., 2014; *Saloranta and Andersen*, 2007], as well as phosphorus loadings, total phosphorus and algae concentrations in eutrophic Norwegian lakes [*Couture et al*., 2014; *Romarheim et al*., 2015]. A module simulating the bacterial decay of DOC was added to the model and used to simulate carbon dynamics in a Finnish lake [*Holmberg et al*., 2014]. The module relies on a 3G approach to OM degradation using parameters from *Vähätalo et al*. [2010]. As defined by *Arndt et al*. [2013], the 3G approach assumes that OM is composed of three discrete compound classes, each characterized by a specific degradability and reactivity toward bacterial mineralization.

The current version of MyLake thus handles ice dynamics, primary productivity, DOC degradation, and the effect of colored dissolved organic matter on light attenuation. This provides a suitable basis to model DO dynamics in humic boreal lakes [*Fang and Stefan*, 2009]. Here we implement key processes in MyLake for DO dynamics and for the early diagenesis of OM in the sediment, as described below, and refer to these changes collectively as MyLake v.2.

2.7. Oxygen Module

Physical exchanges of DO between air and water were added to the model based on *Staehr et al*. [2010]. Briefly, at the lake surface, oxygen exchange between the atmosphere and the water column is calculated from DO saturation and the piston velocity, a function of the wind speed [*Cole and Caraco*, 1998]. DO in the lake is controlled by the balance between photosynthetic production and respiratory consumption. DO production during photosynthesis is proportional to the O_2 yield coefficient of 120 mg O_2 per milligram Chl *a* [*Fang and Stefan*, 2009], building on the first-order kinetic formulation for photosynthesis used in MyLake v.1.2 [*Saloranta and Andersen*, 2007]. DO is also supplied to the lake by stream inflows, which are assumed to be at saturation with respect to atmospheric O_2 concentrations of 21%, as calculated daily as a function of T_{Water} and air pressure [*Benson and Krause*, 1984]. DOC is provided by stream inflows and consumed via photodegradation and biodegradation [*Holmberg et al*., 2014], the latter process consuming DO. Under ice oxygen supply from the atmosphere is assumed by be zero [*Hemmingsen*, 1959], and oxygen supersaturation at the ice-water interface, due to O_2 exclusion during ice formation [*White et al*., 2008], is neglected. Equations implemented in the DO module are given in the SI and references therein.

2.8. Sediment Diagenesis Module

Sediment resuspension, focusing, and heat exchange is calculated on an area-weighted basis, assuming that the difference in area between two successive water column layers consists of sediment area [*Saloranta and Andersen*, 2007]. Sediment-water interactions are handled by coupling MyLake to an existing package that simulates nonsteady state carbon diagenesis in sediments [*Couture et al*., 2010]. Fluxes of settling particles and the concentrations of bottom water dissolved species are provided by MyLake and passed as boundary conditions to the sediment-diagenetic module, which considers only the hypolimnion. Our approach is similar to that of *Smits and van Beek* [2013], who used a process-based sediment diagenesis module rather than empirical sediment-oxygen demand (SOD) module [*Fang and Stefan*, 2009; *Rucinski et al*., 2014].

The sediment diagenesis module comprises a coupled transport-reaction scheme describing kinetic (e.g., microbially mediated primary redox reactions) and equilibrium expressions (e.g., the carbonate system). The reaction network (Table S1) describes the degradation of OM via oxic respiration, denitrification, and sulfate reduction. Consumption of terminal electron acceptors (TEA: e.g., O_2 and NO_3) is coupled to the rate of OM oxidation through a Michaelis-Menten kinetic dependency on the TEA concentration and an inhibition term limiting the rate of a respiratory pathway in the presence of stronger oxidants [*Canavan et al*., 2006]. Secondary O_2 consumption pathways include the oxidation of Fe^{2+}, NH_4^+, and of H_2S and were implemented using bimolecular reaction rate laws and parametrized using default literature values [*Couture et al*., 2010]. Fluxes of dissolved species are the sum of diffusive, advective, and nonlocal transport fluxes, while those of solid species are advective and proportional to particle concentration in the water column and their settling velocity [*Boudreau*, 1997]. The settling particles originate from two sources: (1) autochthonous biomass from decaying primary producers [*Saloranta and Andersen*, 2007] and (2) flocculation of allochthonous DOC [*von Wachenfeldt and Tranvik*, 2008; *von Wachenfeldt et al*., 2008]. In terms of the pools defined

by the 3G approach to OM degradation (see section 2.6), fluxes of autochthonous OM (e.g., settling phytoplankton) were ascribed to labile OM (OM_1 in Table S2), and fluxes of allochthonous OM (e.g., DOC) to semilabile OM pool (OM_2 in Table S2). The measured sediment porosity, decreasing from 0.97 at the sediment-water interface to 0.94 at 25 cm depth, was imposed throughout the calculations. Bioirrigation and bioturbation were both turned off given the low chironomids density of < 10 animals m^{-2} in profundal sediments [*Lindholm et al.*, 2014].

2.9. Model Setup

The model consists of an overarching MATLAB script controlling three individual setups of MyLake: one for each lake basins, chained from upstream to downstream. Each model in the chain receives inputs as follows: (1) the southern basin receives direct and diffuse inflowing water from its local subcatchment, (2) the central basin receives the outflow from the southern basin and diffuse inflowing water, and (3) the northern basin receives the outflow from the central basin and the direct and diffuse inflowing water from its local catchment. Mixing of lake and stream water is calculated at run time.

2.10. Parameter Estimation

Parameter values were estimated by a Bayesian inference algorithm which converges on acceptable parameter sets: the Markov chain Monte Carlo self-adaptive differential evolution learning scheme (MCMC-DREAM) [*Vrugt et al.*, 2009]. It has previously been implemented in MATLAB [*Jackson-Blake and Starrfelt*, 2015; *Starrfelt and Kaste*, 2014] and configured for MyLake [*Couture et al.*, 2014]. The parametrization was performed over the time period 2010–2014 using data for T_{Water} and DO (at 1 m and 8 m depths). Because of the variability in the T_{Water} and DO time series, and given that only 4 years of data were available, we trained the MCMC-DREAM algorithm against the entire time series. Site-specific parameters were allowed to vary within the parameter space bound by prior knowledge. The algorithm was executed over 16 concurrent DREAM chains until the value of the Gelman-Rubin statistics was lower than 1.2 for all chains, after 10^5 iterations. The median simulation among the simulations based on these converged chains of parameter sets was used here as the single-parameterized model. Additional support for the parametrized model was sought by evaluating it against time series of ice phenology over the time period 1974–2014.

Values for other objective functions were calculated to provide alternative performance metrics, although those were not used during calibration: (1) r^2, to quantify the linear relationship between simulated and measured data, (2) the dimensionless Nash-Sutcliffe (NS) statistics which provide a relative model evaluation assessment [*Moriasi et al.*, 2007], (3) the normalized bias (B*, where asterisk denotes normalization), and (4) the normalized unbiased root-mean-square difference (RMSD′*, where apostrophe denotes the removal of bias). Plotting B* against RMSD′* for each pair of observed and modeled time series provides an aggregated model assessment [*Los and Blaas*, 2010] (See Figure S4).

2.11. Scenarios for DO Backcast

The model was used to backcast the response of DO in the epilimnion and in the hypolimnion to increasing DOC concentrations and to increasing T_{Air} for the time period 1974–2014. Scenarios were prepared by subtracting a Sen-slope [*Sen*, 1968] calculated using annual means from the time series of T_{Air} and DOC, yielding a detrended signal that preserves the seasonal dynamics (e.g., Figure S2). Significance of the slopes was established using a Mann-Kendall nonparametric test [*Libiseller and Grimvall*, 2002] on annual means. Using annual means reduced the autocorrelation in the time series and fulfilled the assumption of independence underpinning the Mann-Kendall test. Four scenarios were performed (1) in the "Baseline" scenario both historically increasing T_{Air} and DOC time series were replaced by linearly detrended ones, (2) in the "T_{Air} increase" scenario only DOC time series was detrended, leaving the increasing T_{Air} intact, (3) conversely, in the "DOC increase" scenario only the T_{Air} time series was detrended, leaving the increasing DOC intact, and finally, (4) the "Historical" scenario refers to the scenario where both observed T_{Air} and DOC time series are used.

3. Results

3.1. Trends in Temperature and Catchment Inputs of DOC

Mean annual T_{Air} at Langtjern increased significantly ($p < 0.0002$) between 1970 and 2012 with a Sen-slope of 0.045°C yr^{-1}. Air temperature varied seasonally from 19°C in the summer to −21°C in the

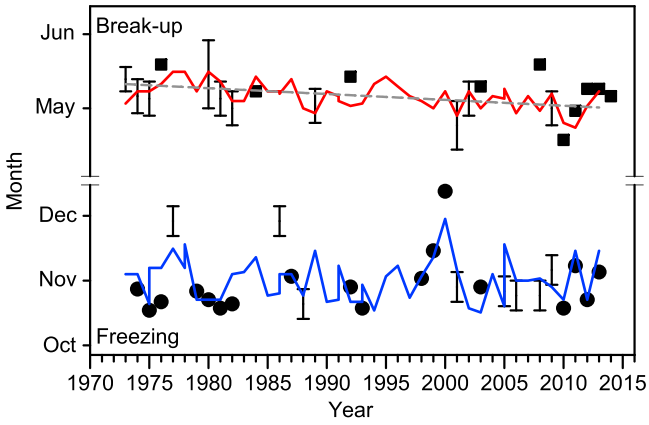

Figure 2. Observed (symbols) and modeled (lines) ice breakup (squares) and freezing dates (circles) at Lake Langtjern for the observation period 1974–2014. The dashed line indicates the trend calculated using model predictions, and error bars represent intervals within which breakup or freezing occurred but was not directly observed. That is, if ice was present at a given date and absent 7 days later, an error bar spanning 7 days is represented in place of a symbol for the breakup date.

winter and spring (Figure S3). Mean annual DOC increased at Langtjern by about 22% over the entire period (calculated as the difference between mean DOC in 1986–1988 and 2011–2014). Similarly, a Sen-slope fitted to DOC concentrations from 1986 to 2014 revealed an increase of 0.11 mg C L^{-1} yr^{-1} during this time period ($p < 0.0001$), similar to the values of 0.13 mg C L^{-1} yr^{-1} reported by *De Wit et al.* [2007] for the period 1985 to 2007. DOC concentrations in the outlet stream (1986–2013) from the catchment varied seasonally from ~6.5 C mg L^{-1} during snowmelt in spring to ~13 mg C L^{-1} in the late autumn and winter (Figure S3). The difference between the seasonal minimum and maximum concentrations of DOC is considerably larger than the magnitude of the long-term trend. Meanwhile, concomitant long-term changes in runoff were not observed (slope = 0.009 m^3 yr^{-1}, $p > 0.02$).

3.2. Ice

The mean freezing date over the past 40 years was 30 October. Ice breakup occurred around mid-May in the 1970s and in the beginning of May in the recent years (Figure 2). Personal communications from site visits suggest that breakup is occurring earlier now than in the early 1970s, but the observation record is too fragmentary to allow robust trend analysis. Instead, ice phenology predicted by MyLake will be used for that purpose (see section 4.1).

3.3. Lake Water Temperature

Observed T_{Water} (2010–2014) in Lake Langtjern is characteristic of dimictic lakes (Figure 3). During open-water periods after spring turnover, surface T_{Water} warmed, peaking at 17.8 – 22.2°C toward the end of July. The T_{Water} decreased afterward until fall turnover, which occurred in late October. During ice cover period, surface water progressively cooled down to 1.5 – 3.6°C until spring turnover. At 8 m depth, bottom T_{Water} increased steadily through the summer from 4.6 to 6.4°C before fall turnover. Bottom T_{Water} under ice cover was stable at 4.0°C throughout the winter period. During the day of ice breakup, the water column was briefly isothermal at 4.0°C, as was also observed by *Pierson et al.* [2011], a phenomenon followed by a rapid increase in surface T_{Water} and the establishment of a thermocline.

3.4. Dissolved Oxygen

DO concentrations in the surface waters at 1 m depth reached 10 mg L^{-1} during both the spring and fall turnovers (Figure 3). The concentrations followed a V-shaped pattern during summer months, decreasing steadily and reached minimum values of 2.4–6.1 mg L^{-1} during short-lived oxygen depletion episodes occurring during the warmest days; DO then increased again as the lake cooled down toward fall turnover. Under ice cover, DO decreased to different plateaus depending on the year. Immediately following spring turnover, surface water DO peaked at 11.2–11.7 mg L^{-1}. In the bottom waters at 8 m depth, DO concentration reached 10 mg L^{-1} just before freezing, then decreased steadily under the ice. Anoxia was observed under the ice cover for all years. DO increased immediately after ice breakup in the spring, but the DO level varied strongly between years, from 2 mg L^{-1} in 2011 to 10 mg L^{-1} in 2013. A steady decrease in DO at 8 m depth occurred every summer, but whether hypoxia (<3 mg DO L^{-1}) was reached appears to depend on the extent of the ventilation of the water column after spring turnover (Figure 3c). In the summer, bottom water DO generally decreased steadily: the hypolimnion became anoxic in 2011, hypoxic in 2010 and 2012, and remained oxygenated in 2013.

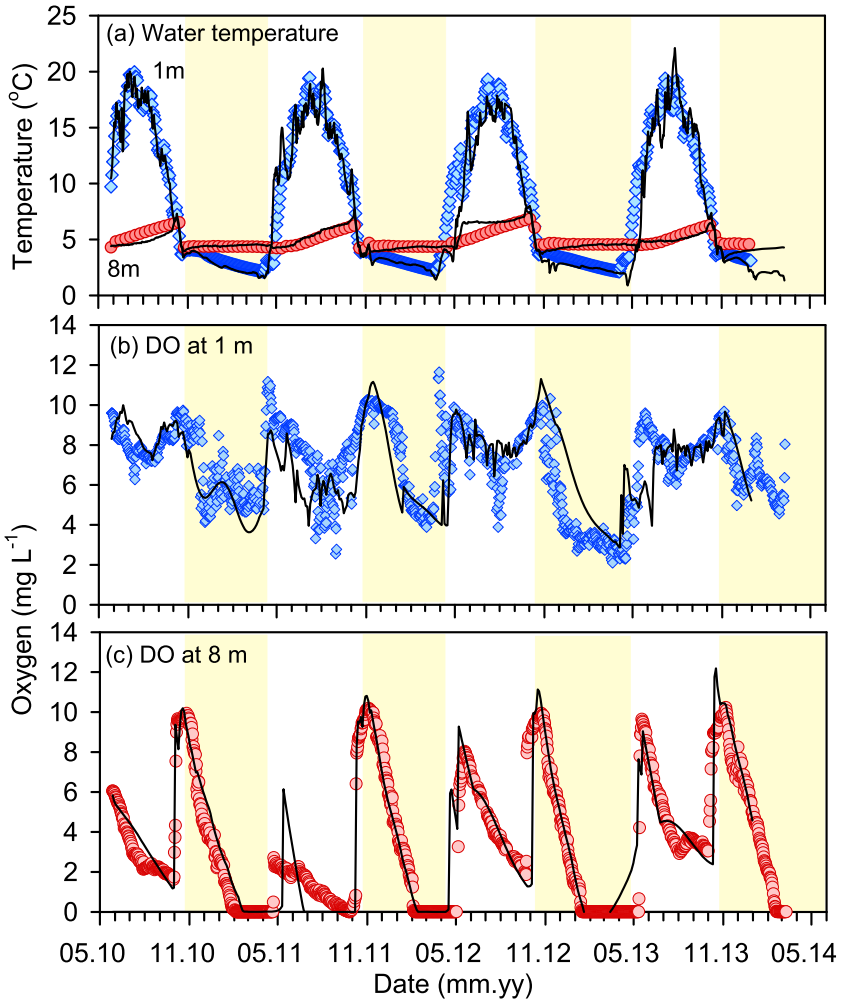

Figure 3. Daily average of observed (symbols) and simulated (lines) (a) water temperature and (b) DO in surface and (c) bottom water of the Northern basin of Lake Langtjern for the model parametrization period 27 May 2010 to 27 May 2014. The shaded areas indicate ice cover period.

3.5. Model Performance

Convergence of the MCMC-DREAM chains indicates that the parameters were probably calibrated to the global maximum within the prior parameter space. Performance indicators of the model are shown in Table 2. Overall, values of r^2, root-mean-square error (RMSE), and NS testify to good model performance

Table 2. Summary of Model Performance Statistics for Parametrization and Evaluation Calculated Using the Median Model of the MCMC-DREAM Calibration[a]

Parameter		n	r^2	RMSE	NS	RMSD'*	B*
			Model Parametrization (2010–2014)				
Temperature	1 m	1384	0.74	0.02°C	0.56	−0.71	9×10^{-3}
Temperature	8 m	1384	0.85	0.01°C	0.82	0.54	5×10^{-2}
Oxygen	1 m	1384	0.69	1.70 mg L^{-1}	0.58	−0.71	-6×10^{-2}
Oxygen	8 m	1384	0.76	1.67 mg L^{-1}	0.63	−0.66	8×10^{-3}
			Model Evaluation (1974–2014)				
Freezing date		26	0.76	0.48 d	0.68	−0.69	0.12
Breakup date		21	0.92	1.55 d	0.92	−0.38	0.10

[a]Coefficient of determination (r^2), root-mean-square error (RMSE), Nash-Sutcliffe coefficient (NS), normalized unbiased root-mean-square difference (RMSD'*), and normalized bias (B*) for temperature and oxygen at 1 m and 8 m depths and for ice freezing and breakup dates.

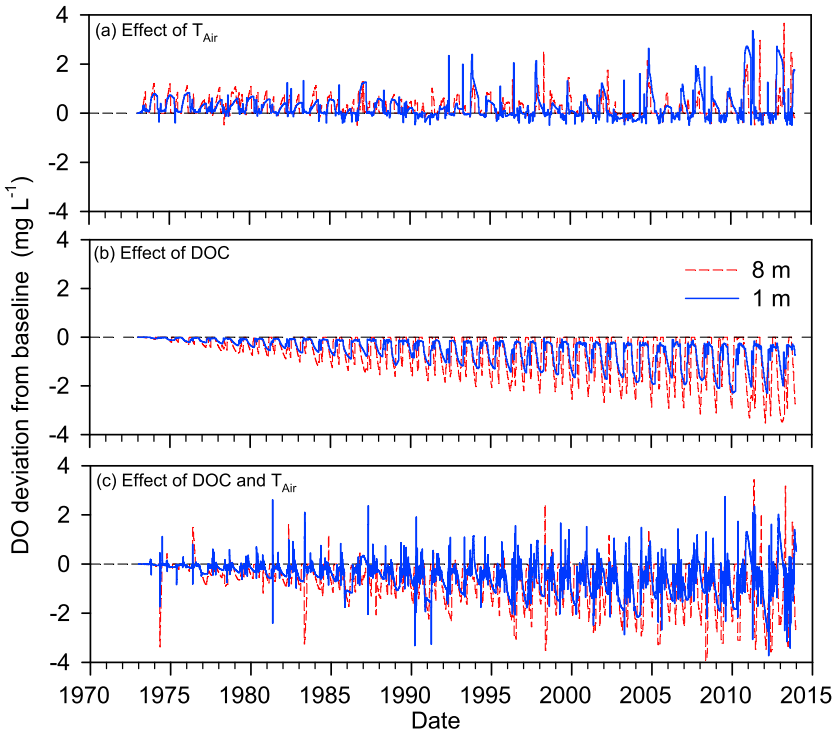

Figure 4. Net effect of increasing (a) T_{Air}, (b) DOC, and of (c) both T_{Air} and DOC on DO concentrations at 1 m (solid lines) and 8 m (dashed lines) depth in Lake Langtjern calculated by subtracting the results of the baseline simulations for which neither T_{Air} nor DOC is increasing.

[*Moriasi et al.*, 2007]. B* values indicate that simulations are unbiased, that is, the model does not systematically overestimate or underestimate the observations. RMSD'* values further indicate that the standard deviation (σ) of simulated values is smaller than that of the observations for all variables except T_{Water} simulated at 8 m depth (Table 2). Observed spring and summer T_{Water} are well reproduced, as the model captures the temporal patterns and the timing of the water column turnover. Simulated oxygen time series are unbiased, and their variance is similar to that of the observations. The performance of the model is lower for DO at 1 m than at 8 m depth (Figures 3 and S3, Table 2, and section 4.2). In particular, at 1 m depth there are mismatches in the magnitude of ventilation events during spring and fall turnover, and of the short-lived DO depletion events in the summer at the lake's surface. Ice phenology is reproduced well by the model, and the RMSE for simulated freezing and ice breakup dates is low.

3.6. Effect of Increasing Air Temperature and DOC on DO Concentrations

Four scenarios were tested to illustrate the net effect of T_{Air} and DOC on DO concentrations. The results of the historical simulation, of the T_{Air} increase, and of the DOC increase scenario were subtracted from the results of the Baseline scenario (Figure 4). This shows that increasing T_{Air} resulted in increasingly higher DO concentrations throughout the simulation period of 1974–2014, when compared to the baseline, amounting to a maximum increase of 2 and ~4 mg DO L^{-1} in epilimnion and hypolimnion, respectively (Figure 4a). In contrast, increasing DOC resulted in a steady decline of DO. The increase of DOC concentration led to a decline of 2 and ~3.5 mg DO L^{-1} in the epilimnion and hypolimnion, respectively (Figure 4b). The Historical scenario, which combines the observed increase in T_{Air} and in DOC, showed that these two drivers of DO resulted in a net decrease in DO in both the epilimnion and the hypolimnion (Figure 4c).

Daily simulated DO values were averaged over 40 years, for each Julian day in a year, to further examine the intraannual response of DO to increasing T_{Air} and DOC. This produced a sequence of 365 means (ignoring 29 February in leap years), with sample size $n = 40$ (Figure 5). The effect of increasing T_{Air} on DO depended on the season: under the "T_{air}" scenario, DO increased throughout the fall, winter, and early spring in both the epilimnion and hypolimnion, while it sharply decreased in the hypolimnion in late summer (Figure 5d).

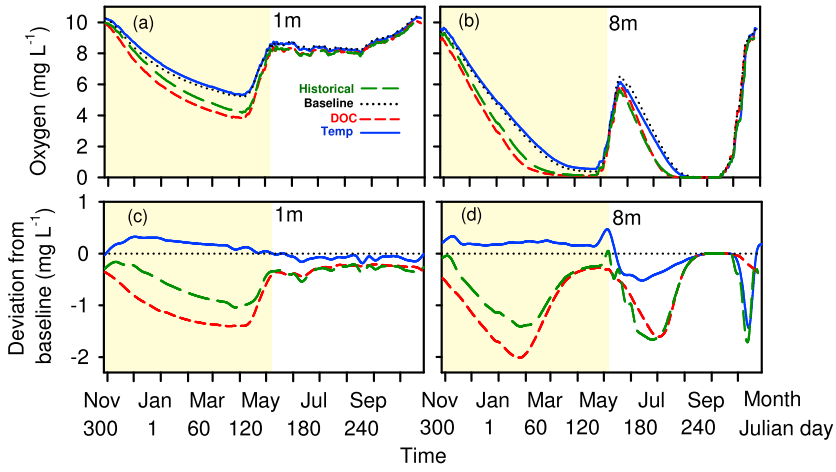

Figure 5. Average DO concentrations for the period of 1974–2014 predicted for each Julian day, starting at the lake freezing date, simulated using measured increasing T_{Air} and DOC (i.e., Historical, long dashed), detrended T_{Air} and DOC time series (i.e., Baseline, dotted line), and with either T_{Air} increase (solid line) or DOC increase (dashed line) at the (a) 1 m and (b) 8 m depths. Values normalized against the Baseline simulations show the net effect of increasing temperature, DOC, or both at (c) 1 m and (d) 8 m depth. Shaded areas indicate ice cover periods.

The increase in DOC had a negative effect on DO throughout the year, but the decline in DO was more pronounced under ice cover and in the period leading up to anoxia in the hypolimnion in the midsummer. The more DOC, the faster was the decline in DO. Finally, all simulations showed relatively similar DO values during spring and fall turnovers (Figures 5a and 5b), which is an indication of yearly resetting of DO concentration profiles in the water column.

4. Discussion

4.1. Trends in Air Temperature, Ice Phenology, and DOC

Trends observed in T_{Air} and ice phenology at Langtjern agree with what is observed at the larger scale. The increase in T_{Air} measured at Langtjern (0.045°C yr^{-1}) for the period 1970–2012 is close to the reported regional climate warming for southeast Norway [*Hanssen-Bauer*, 2005] of 0.039°C yr^{-1} for 1965–2004. The 1970–2012 trend suggests faster warning than the long-term 1875–2004 trend of 0.011°C yr^{-1} in the same region. Climate warming in the twentieth century has been most pronounced in the spring and fall season in Scandinavia [*Zveryaev and Gulev*, 2009] and in southeast Norway [*Hanssen-Bauer*, 2005].

At Lake Langtjern, the observed ice record is sparse. The model allows us to fill this data gap by integrating 40 years of atmospheric and hydrologic forcings with existing ice observations (Figure 2). A trend toward early ice breakup dates (-0.25 d yr^{-1}; $p < 0.002$) is found in the model-predicted ice phenology, which can be related to the increasing T_{Air} [*Dibike et al.*, 2012; *Johnson and Stefan*, 2006]. In contrast, there is no significant trend in ice freezing dates. This is consistent with ice phenology observed throughout Fennoscandia [*Duguay et al.*, 2013] where a shortening of ice coverage is generally observed. However, not all lakes were subjected to early breakup, as trends in the duration of ice cover vary depending on altitude. Increased precipitation occurs together with increased in T_{Air} leading to thicker snow cover [*Šporka et al.*, 2006]. As a result, lake ice cover decreased in southern part of Fennoscandia, where Langtjern lies, while the opposite tendency was found in the north throughout the period of 1936–2000 [*Baltic Earth Assessment of Climate Change*, 2008].

Temperature and discharge have explained seasonal and interannual variations in DOC at Langtjern [*De Wit et al.*, 2007]. The increase in DOC observed over the past 30 years at Lake Langtjern is characteristic of a large-scale phenomenon occurring in boreal catchments [*Monteith et al.*, 2007]. The hypothesized mechanism behind the widespread increase in DOC is the enhanced mobilization of soil OM in response to reduced acid deposition, through the complex interplay between the solubility of humic acids, soil pH, and the soil ionic strength [*De Wit et al.*, 1999, 2007]. Model projections of DOC in boreal lakes suggest that hydrology (i.e., droughts and floods), rather than acid deposition, will impact future trends in DOC [*Holmberg et al.*, 2014].

Given the strong relation between discharge and DOC export, a continuing increase of aquatic DOC export from catchments seems likely [*Wilson et al*., 2010] as a combined effect of positive trends in DOC and increases in discharge due to climate change [*Raike et al*., 2012]. As DOC in surface waters increases, less light penetration in the water column might hamper autochthonous production of organic carbon, thus increasing the role of DOC in aquatic food webs via the microbial loop [*Finstad et al*., 2014]. Yet because climate change could result in more variable weather, it is possible that DOC in boreal lakes will be more variable in the future than in the past.

4.2. Sources of Uncertainty

Simulated DO values have either less variance (at 8 m) or more variance (at 1 m) than the observations, suggesting that aspects of the DO dynamics are not fully captured by the model particularly at the lake's surface (Table 2). Keeping in mind that singling out specific reasons for mismatches is speculative when modeling dynamic systems [*Fang and Stefan*, 2009], it is likely that the high-frequency DO sensor responds to convective mixing across a stratified layer, to horizontal exchange of DO with the shallow littoral zone [*Staehr et al*., 2010], or to internal waves [*Kirillin et al*., 2012]. These phenomena are not captured by a 1-D model with a daily time step. On the other hand, better model performance for DO at 8 m than at 1 m depth (Table 2) suggests that DO consumption via DOC degradation in the hypolimnion [*Stefanovic and Stefan*, 2002] and sediment respiration are well constrained (Figure 3).

Further, uncertainty in the temporal variation of the DO saturation of inflowing streams may have impacted the model results. Specifically, the assumption that DO in the streams is at equilibrium with the atmosphere may not hold if primary productivity leads to oversaturated inflows, or if respiration and seepage of DO-depleted groundwater into the lake lead to undersaturated inflows. In the absence of measurements of stream DO, we tested the response of the model to deviations of ±40% with respect to theoretical saturation values, which have been reported in streams [*Chen et al*., 2014]. The model forecasts average changes of −26% and +34 % in water column DO, as a response to a change in inflow of DO of −40% or +40%, respectively. Nevertheless, because DO saturation was shown to be a reasonable assumption for daily averages in cold streams [*Demars et al*., 2011], we do not expect that this sensitivity will impact the direction or magnitude of the changes in DO predicted by the model.

Finally, uncertainty in the model predictions may stem from the representation of sediment processes. First, the module averages sediment properties within the hypolimnion. The spatial representation of sediment diagenesis in lake models is an enduring challenge [*Gal et al*., 2014], and to our knowledge it has not been implemented in 1-D models and only rarely in 3-D lake models [*Frassl et al*., 2014; *Smits and van Beek*, 2013]. Instead, a single sediment column is the most commonly used representation of diagenesis when sediment modules are two-way coupled with the water column [*Paraska et al*., 2014], in part because most of the 1-D modeling efforts have historically been dedicated to marine settings [*Peña et al*., 2010]. This is the approach we have selected here as it allows accounting for sediment diagenesis while retaining key features of 1-D models such as speed of execution, flexibility, and suitability for autocalibration and sensitivity analysis [*Gelda et al*., 2013]. Second, methane (CH_4) production in the sediment and its aerobic oxidation is not included in the reaction network, which may lead to an overestimation of other O_2-consuming processes because CH_4 oxidation can be a significant DO sink in lakes [*Maeck et al*., 2013; *Maerki et al*., 2009; *Schwarz et al*., 2008]. However, CH_4 oxidation in oligotrophic boreal lakes is lower than in eutrophic lakes [*Bretz and Whalen*, 2014], because of the lack of strong seasonal pulses of autochthonous carbon (i.e., algal blooms) to fuel CH_4 production [*Schwarz et al*., 2008]. For example, *Algesten et al*. [2005] reported an average summer CH_4 production rate, in the sediments of 15 oligotrophic lakes, of ~0.4 mmol CH_4 m^{-2} d^{-1}. In comparison, model-predicted DO consumption in the sediment at Lake Langtjern is ~12 mmol O_2 m^{-2} d^{-1}, thus thirtyfold higher than the potential CH_4 production rates. Such a low contribution of CH_4 oxidation to DO consumption at the sediment-water interface contrasts with findings for eutrophic lakes, where it can account for 39–56% of DO removal [*Maerki et al*., 2009]. As a result, our model structure would need adaptation for applications in eutrophic lakes and in the event that boreal lakes get warmer and more productive in the future, thus producing more CH_4.

4.3. Controls on DO Dynamics

The model results suggest that diminishing ice cover duration enhances spring oxygenation of the water column (Figure 4a). At the same time, as T_{Air} warming trends strengthen, the lake changes toward a more

Table 3. Number of Days yr^{-1} and Total Number of Events During Which Water Column DO Concentrations at 1 m and 8 m Depths Remained Below the Thresholds for Hypoxia (3 mg L^{-1}, Affecting Fish) and Anoxia (16 µg L^{-1}, Affecting Microbial Metabolism) in Scenarios Using Measured Increasing T_{Air} and DOC (i.e., Historical), Linearly Detrended T_{Air} and DOC Time Series (i.e., Baseline), or Either T_{Air} Increase or DOC Increase[a]

Input Time Series	Criteria		1 m	8 m
Baseline (detrended DOC + T_{Air})	anoxia	Days yr^{-1}	0	102
		Events #	0	65
	hypoxia	Days yr^{-1}	0	209
		Events #	0	81
Historical (observed DOC + T_{Air})	anoxia	Days yr^{-1}	0	163
		Events #	0	76
	hypoxia	Days yr^{-1}	7	244
		Events #	6	79
T_{Air} increase (detrended DOC + observed T_{Air})	anoxia	Days yr^{-1}	0	107
		Events #	0	67
	hypoxia	Days yr^{-1}	0	210
		Events #	0	77
DOC increase (observed DOC + detrended T_{Air})	anoxia	Days yr^{-1}	0	180
		Events #	0	81
	hypoxia	Days yr^{-1}	14	249
		Events #	13	82

[a]See Figure 4 and 5 for results of these simulations.

temperate type with shorter ice cover period and warmer T_{Water}, both of which enhance microbial activity and reduce DO availability (Figure 5d). Therefore, the current beneficial effect of increasing T_{Air} on boreal lake DO is likely to be compensated for in the longer term by the negative effect of enhanced oxygen demand, as observed by *Jankowski et al*. [2006] for temperate lakes. These predictions of the effect of climate change on DO are in line with those of *Fang and Stefan* [2009], who showed that lake anoxia under ice is projected to shorten, but that the periods of hypolimnetic summer anoxia are projected to lengthen. Later freezing dates might also affect T_{Water} and enhance DO availability. Interestingly, in Lake Päijänne (Finland), the lowest hypolimnetic T_{Water} on record (~1°C) was observed when the lake freezing date was exceptionally late [*Pulkkanen and Salonen*, 2013]. This phenomenon is ascribed to the fact that, in northern latitudes, solar radiation is low in the autumn when ice usually forms, such that delayed freezing allows more time for the cooling of the water and sediment, causing lower under-ice T_{Water} [*Saloranta et al*., 2009] and potentially reducing oxygen demand.

The MyLake model predicts that an increase in DOC is systematically followed by a decline in DO (Figures 4b and 5), leading to an earlier onset of anoxia in the hypolimnion, both under ice and around the midsummer (Figure 5d). DO depletion is mainly driven by heterotrophic microbial processes and, under ice, is often viewed as a zeroth-order reaction leading to a linear DO decrease [*Bertilsson et al*., 2013]. This is what we observed at Lake Langtjern, where DO depletion was linear under ice cover ($r^2 = 0.99$). Using our under-ice DO measurements (Figure 3), we estimated a rate of DO consumption (R_{DO}, mg L^{-1} d^{-1}) of $7.50 \pm 0.05 \times 10^{-2}$. This value falls within the range of 2×10^{-2}–1 mg L^{-1} d^{-1} reviewed by *Terzhevik et al*. [2010] for under-ice DO consumption. Under-ice R_{DO} values calculated using the results of the long-term simulations Baseline, T_{Air} increase and DOC increase are 6.51, 6.34, and 7.50×10^{-2} mg L^{-1} d^{-1}, respectively. The fastest depletion rates are thus found during the DOC increase scenario, and the slowest rates during the T_{Air} increase scenario, suggesting that DOC and higher T_{Air} are antagonistic factors influencing DO concentrations under ice.

5. Implications

Longer periods of anoxia in the hypolimnion and the higher frequency of naturally occurring winter anoxic episodes in lakes have potential impacts on heterotrophic microbial metabolism, fish oxythermal habitat, and drinking water quality. The impact of DOC on the lake ecosystems is unlikely to be limited to lowering DO level anoxia, because colored DOC can impede energy flow in the food webs [*Finstad et al*., 2014]. Still, DOC-controlled anoxia appears to be a chief factor controlling productivity in lakes, as recently discussed

by *Craig et al*. [2015]. This highlights the usefulness of modeling tools able to quantify the response of water column oxygenation to variable DOC loads.

Table 3 summarizes the model-predicted influence of T_{Air} and DOC on oxygen availability for fish and oxygen-respiring microorganisms in Lake Langtjern by showing the total number of hypoxic and anoxic days for each of the four scenarios tested. Two conclusions stand out: (1) increasing only T_{Air} by +1.3°C does not change the number of hypoxic or anoxic days (compared to the baseline scenario), and (2) increasing both T_{Air} and DOC (+22% from 1986 to 2013) leads to shorter hypoxic and anoxic events than when increasing DOC only. Therefore, a shorter ice cover period mitigates the DO decrease brought about by increasing DOC. The model suggests that, thus far, the impact of DOC-driven decrease of DO concentrations has been much larger than the climate-driven shortening of ice cover duration [*Craig et al*., 2015]. Drinking water in boreal regions often comes from surface waters, where high and increasing DOC concentrations cause problems for water treatment in terms of DOC removal [*Hongve et al*., 2004]. If shortening of ice cover duration continues along with increasing of water temperatures and DOC concentrations, hypoxia and anoxia might become more common in Fennoscandian drinking water reservoirs.

The impact of browning and warming on DO in productive lake is likely to be more multifaceted than what is described here for oligotrophic lakes. Factors such as CO_2 concentrations, nutrient availability, and microbial community dynamics will modulate the growth rates of photosynthetic organisms and thus DO production [*Kosten et al*., 2012]. It is expected that algal species such as *Microcystis aeruginosa* [*Paerl and Paul*, 2012] or *Gonyostomum semen* [*Hagman et al*., 2015] will thrive. Anoxic conditions in the hypolimnion of eutrophic lakes can also trigger the release of sediment-bound phosphorus (further sustaining algal growth), the formation of methyl mercury and its accumulation in fish, and the formation of CH_4 which can be released to the atmosphere [*Vuorenmaa et al*., 2014].

Acknowledgments

The data supporting Figures 2 and 3 are freely available at http://www.niva.no/langtjern. The Matlab codes for the MyLake application at Lake Langtjern are freely available at https://github.com/biogeochemistry/Langtjern but access to the repository must be obtained by contacting the corresponding author. R.M.C. acknowledges funding by NFR project "Lakes in Transition" (Research Council of Norway contract 244558/E50) and FP7 EU-MARS (contract 603378). This study was also funded by projects BIWA (RCN contract 221410) and ECCO (RCN contract 224779/E10) as well as by NIVA's Strategic Institute Initiative "Climate effects from Mountains to Fjords" (RCN contract 208279). We are indebted to U. Brandt (NIVA) for installation and maintenance of the lake buoy and of the weather station at Langtjern, K. Sønsteby for collection of weekly water samples and for observation of ice cover, J. Starrfelt (University of Oslo) for provision of MATLAB scripts for MCMC-DREAM analysis, Y. Lin (NIVA) for collating weather data at Langtjern, N. Urban (Michigan Tech) for information on sediment porosity at Lake Langtjern, D. Cossa for provision of writing facilities, and K. Mueller for editing the manuscript. R.M.C. acknowledges discussions during network-level activities of the Networking Lake observatories in Europe (NETLAKE, action ES1201) funded by the European Cooperation in Science and Technology (COST).

References

Algesten, G., S. Sobek, A.-K. Bergström, A. Jonsson, L. Tranvik, and M. Jansson (2005), Contribution of sediment respiration to summer CO_2 emission from low productive boreal and subarctic lakes, *Microb. Ecol.*, *50*(4), 529–535.

Arndt, S., B. B. Jørgensen, D. E. LaRowe, J. J. Middelburg, R. D. Pancost, and P. Regnier (2013), Quantifying the degradation of organic matter in marine sediments: A review and synthesis, *Earth Sci. Rev.*, *123*, 53–86.

Arp, C. D., B. M. Jones, and G. Grosse (2013), Recent lake ice-out phenology within and among lake districts of Alaska, U.S.A, *Limnol. Oceanogr.*, *58*(6), 2013–2028.

Baltic Earth Assessment of Climate Change (2008), *Assessment of Climate Change for the Baltic Sea Basin*, vol. 473, xiii pp., Springer, Berlin.

Benson, B., and D. Krause (1984), The concentration and isotopic fractionation of oxygen dissolved in fresh-water and seawater in equilibrium with the atmosphere, *Limnol. Oceanogr.*, *29*(3), 620–632.

Benson, B., and J. Magnuson (2012), *Global Lake and River Ice Phenology Database*[Freeze/Thaw Subset], edited, National Snow and Ice Data Center, Boulder, Colo.

Bertilsson, S., et al. (2013), The under-ice microbiome of seasonally frozen lakes, *Limnol. Oceanogr.*, *58*(6), 1998–2012.

Blenckner, T., R. Adrian, L. Arvola, M. Järvinen, P. Nõges, T. Nõges, K. Pettersson, and G. Weyhenmeyer (2010), The impact of climate change on lakes in northern Europe, in *The Impact of Climate Change on European Lakes*, edited by G. George, pp. 339–358, Springer, Netherlands.

Blunden, J., and D. S. Arndt (2013), State of the climate in 2012, *Bull. Am. Meteorol. Soc.*, *94*(8), S1–S258.

Boudreau, B. P. (1997), *Diagenetic Models and Their Implementation*, 1st ed., Springer, Berlin.

Bretz, K. A., and S. C. Whalen (2014), Methane cycling dynamics in sediments of Alaskan Arctic Foothill lakes, *Inland Waters*, *4*(1), 65–78.

Brothers, S., K. J. Köhler, K. Attermeyer, H.-P. Grossart, T. Mehner, N. Meyer, K. Scharnweber, and S. Hilt (2014), A feedback loop links brownification and anoxia in a temperate, shallow lake, *Limnol. Oceanogr.*, *59*(4), 1388–1398.

Canavan, R. W., C. P. Slomp, P. Jourabchi, P. Van Cappellen, A. M. Laverman, and G. A. Van Den Berg (2006), Organic matter mineralization in sediment of a coastal freshwater lake and response to salinization, *Geochim. Cosmochim. Acta*, *70*(11), 2836–2855.

Chen, G., J. Venkiteswaran, S. Schiff, and W. Taylor (2014), Inverse modeling of dissolved O2 and δ18O-DO to estimate aquatic metabolism, reaeration and respiration isotopic fractionation: Effects of variable light regimes and input uncertainties, *Aquat. Sci.*, *76*(3), 313–329.

Clilverd, H., D. White, and M. Lilly (2009), Chemical and physical controls on the oxygen regime of ice-covered arctic lakes and reservoirs, *J. Am. Water Resour. Assoc.*, *45*(2), 500–511.

Cole, J. J., and N. F. Caraco (1998), Atmospheric exchange of carbon dioxide in a low-wind oligotrophic lake measured by the addition of SF6, *Limnol. Oceanogr.*, *43*(4), 647–656.

Cooke, G. D., E. B. Welch, S. Peterson, and S. A. Nichols (2005), *Restoration and Management of Lakes and Reservoirs*, 3rd ed., CRC Press, Boca Raton, Fla.

Couture, R.-M., B. Shafei, P. Van Cappellen, A. Tessier, and C. Gobeil (2010), Non-steady state modeling of arsenic diagenesis in lake sediments, *Environ. Sci. Technol.*, *44*(1), 197–203.

Couture, R.-M., K. Tominaga, J. Starrfelt, S. J. Moe, O. Kaste, and R. F. Wright (2014), Modelling phosphorus loading and algal blooms in a Nordic agricultural catchment-lake system under changing land-use and climate, *Environ. Sci. Processes Impacts*, *16*(7), 1588–1599.

Craig, N., S. E. Jones, B. C. Weidel, and C. T. Solomon (2015), Habitat, not resource availability, limits consumer production in lake ecosystems, *Limnol. Oceanogr.*, *60*, 2079–2089, doi:10.1002/lno.10153.

De Wit, H. A., M. Kotowski, and J. Mulder (1999), Modeling aluminum and organic matter solubility in the forest floor using WHAM, *Soil Sci. Soc. Am. J.*, *63*(5), 1141–1148.

De Wit, H. A., J. Mulder, A. Hindar, and L. Hole (2007), Long-term increase in dissolved organic carbon in streamwaters in Norway is response to reduced acid deposition, *Environ. Sci. Technol.*, *41*(22), 7706–7713.
De Wit, H. A., A. Hindar, and L. Hole (2008), Winter climate affects long-term trends in stream water nitrate in acid-sensitive catchments in southern Norway, *Hydrol. Earth Syst. Sci.*, *12*(2), 393–403.
De Wit, H. A., A. Granhus, M. Lindholm, M. J. Kainz, Y. Lin, H. F. V. Braaten, and J. Blaszczak (2014), Forest harvest effects on mercury in streams and biota in Norwegian boreal catchments, *For. Ecol. Manage.*, *324*, 52–63.
Demars, B. O. L., J. Russell Manson, J. S. Ólafsson, G. M. Gislason, R. Gudmundsdottir, G. U. Y. Woodward, J. Reiss, D. E. Pichler, J. J. Rasmussen, and N. Friberg (2011), Temperature and the metabolic balance of streams, *Freshwater Biol.*, *56*(6), 1106–1121.
Dibike, Y., T. Prowse, B. Bonsal, L. D. Rham, and T. Saloranta (2012), Simulation of North American lake-ice cover characteristics under contemporary and future climate conditions, *Int. J. Climatol.*, *32*(5), 695–709.
Dillon, P. J., B. J. Clark, L. A. Molot, and H. E. Evans (2003), Predicting the location of optimal habitat boundaries for lake trout (*Salvelinus namaycush*) in Canadian Shield lakes, *Can. J. Fish. Aquat. Sci.*, *60*(8), 959–970.
Downing, J. A., et al. (2006), The global abundance and size distribution of lakes, ponds, and impoundments, *Limnol. Oceanogr.*, *51*(5), 2388–2397.
Duguay, C., L. Brown, K.-K. Kang, and H. Kheyrollah Pour (2013), Arctic - Lake ice, in State of the Climate in 2012, *Bull. Am. Meteorol. Soc.*, *94*(8), S124–S126.
Fang, X., and H. G. Stefan (2009), Simulations of climate effects on water temperature, dissolved oxygen, and ice and snow covers in lakes of the contiguous United States under past and future climate scenarios, *Limnol. Oceanogr.*, *54*(6), 2359–2370.
Fee, E. J., R. E. Hecky, S. E. M. Kasian, and D. R. Cruikshank (1996), Effects of lake size, water clarity, and climatic variability on mixing depths in Canadian Shield lakes, *Limnol. Oceanogr.*, *41*(5), 912–920.
Finstad, A. G., I. P. Helland, O. Ugedal, T. Hesthagen, and D. O. Hessen (2014), Unimodal response of fish yield to dissolved organic carbon, *Ecol. Lett.*, *17*(1), 36–43.
Frassl, M. A., K.-O. Rothhaupt, and K. Rinke (2014), Algal internal nutrient stores feedback on vertical phosphorus distribution in large lakes, *J. Great Lakes Res.*, *40*, 162–172.
Futter, M. N., and H. A. de Wit (2008), Testing seasonal and long-term controls of streamwater DOC using empirical and process-based models, *Sci. Total Environ.*, *407*(1), 698–707.
Gal, G., M. Hipsey, K. Rinke, and B. Robson (2014), Novel approaches to address challenges in modelling aquatic ecosystems, *Environ. Modell. Software*, *61*, 246–248.
Garmo, Ø., et al. (2014), Trends in surface water chemistry in acidified areas in Europe and North America from 1990 to 2008, *Water Air Soil Pollut.*, *225*(3), 1–14.
Gebre, S., T. Boissy, and K. Alfredsen (2014), Sensitivity of lake ice regimes to climate change in the Nordic region, *Cryosphere*, *7*(8), 1589–1605.
Gelda, R., E. Owens, D. Matthews, S. Effler, S. Chapra, M. Auer, and R. Gawde (2013), Modeling effects of sediment diagenesis on recovery of hypolimnetic oxygen, *J. Environ. Eng.*, *139*(1), 44–53.
Golosov, S., A. Terzhevik, I. Zverev, G. Kirillin, and C. Engelhardt (2012), Climate change impact on thermal and oxygen regime of shallow lakes, *Tellus A*, *64*, doi:10.3402/tellusa.v64i0.17264.
Hagman, C. H. C., A. Ballot, D. O. Hjermann, B. Skjelbred, P. Brettum, and R. Ptacnik (2015), The occurrence and spread of *Gonyostomum semen* (Ehr.) Diesing (Raphidophyceae) in Norwegian lakes, *Hydrobiologia*, *744*(1), 1–14.
Hanssen-Bauer, I. (2005), Regional temperature and precipitation series for Norway: Analyses of time-series updated to 2004. *Rep.*, *Report nr. 2005/15*, 34 pp., Norwegian Meterological Institute, Oslo.
Hemmingsen, E. (1959), Permeation of gases through ice, *Tellus*, *11*(3), 355–359.
Henriksen, A., B. L. Skjelvåle, J. Mannio, A. Wilander, H. Ron, C. Curtis, J. P. Jensen, E. Fjeld, and T. Moiseenko (1998), Northern European Lake Survey, 1995: Finland, Norway, Sweden, Denmark, Russian Kola, Russian Karelia, Scotland and Wales, *AMBIO*, *27*(2), 80–91.
Holmberg, M., M. N. Futter, N. Kotamäki, S. Fronzek, M. Forsius, P. Kiuru, N. Pirttioja, K. Rasmus, M. Starr, and J. Vuorenmaa (2014), Effects of changing climate on the hydrology of a boreal catchment and lake DOC—Probabilistic assessment of a dynamic model chain, *Boreal Environ. Res.*, *19*(suppl. A), 66–82.
Hondzo, M., and H. Stefan (1993), Lake water temperature simulation model, *J. Hydraul. Eng.*, *119*(11), 1251–1273.
Hongve, D., G. Riise, and J. F. Kristiansen (2004), Increased colour and organic acid concentrations in Norwegian forest lakes and drinking water—A result of increased precipitation?, *Aquat. Sci.*, *66*(2), 231–238.
ICP Waters (2010), ICP Waters Programme Manual 2010, *Rep.*, *105/2010*, 91 pp., ICP Waters, Oslo.
Jackson-Blake, L., and J. Starrfelt (2015), Do higher data frequency and Bayesian auto-calibration lead to better model calibration? Insights from an application of INCA-P, a process-based river phosphorus model, *J. Hydrol.*, *527*, 641–655.
Jankowski, T., D. M. Livingstone, H. Buhrer, R. Forster, and P. Niederhauser (2006), Consequences of the 2003 European heat wave for lake temperature profiles, thermal stability, and hypolimnetic oxygen depletion: Implications for a warmer world, *Limnol. Oceanogr.*, *51*(2), 815–819.
Jiang, L. P., X. Fang, H. G. Stefan, P. C. Jacobson, and D. L. Pereira (2012), Oxythermal habitat parameters and identifying cisco refuge lakes in Minnesota under future climate scenarios using variable benchmark periods, *Ecol. Modell.*, *232*, 14–27.
Johnson, S., and H. Stefan (2006), Indicators of climate warming in Minnesota: Lake ICE covers and snowmelt runoff, *Clim. Change*, *75*(4), 421–453.
Kheyrollah Pour, H., C. Duguay, A. Martynov, and L. C. Brown (2012), Simulation of surface temperature and ice cover of large northern lakes with 1-D models: A comparison with MODIS satellite data and in situ measurements, *Tellus A*, *64*, doi:10.3402/tellusa.v64i0.17614.
Kirillin, G., et al. (2012), Physics of seasonally ice-covered lakes: A review, *Aquat. Sci.*, *74*(4), 659–682.
Kosten, S., et al. (2012), Warmer climates boost cyanobacterial dominance in shallow lakes, *Global Change Biol.*, *18*(1), 118–126.
Kothawala, D. N., C. A. Stedmon, R. A. Müller, G. A. Weyhenmeyer, S. J. Köhler, and L. J. Tranvik (2014), Controls of dissolved organic matter quality: Evidence from a large-scale boreal lake survey, *Global Change Biol.*, *20*(4), 1101–1114.
Kraal, P., E. D. Burton, A. L. Rose, M. D. Cheetham, R. T. Bush, and L. A. Sullivan (2013), Decoupling between water column oxygenation and benthic phosphate dynamics in a shallow eutrophic estuary, *Environ. Sci. Technol.*, *47*(7), 3114–3121.
Libiseller, C., and A. Grimvall (2002), Performance of partial Mann-Kendall tests for trend detection in the presence of covariates, *Environmetrics*, *13*(1), 71–84.
Lindholm, M., H. A. De Wit, T. E. Eriksen, and H. F. V. Braaten (2014), The influence of littoral on Mercury bioaccumulation in a humic lake, *Water Air Soil Pollut.*, *225*(10), doi:10.1007/s11270-014-2141-4.

Livingstone, D. M., and R. Adrian (2009), Modeling the duration of intermittent ice cover on a lake for climate-change studies, *Limnol. Oceanogr.*, *54*(5), 1709.
Los, F. J., and M. Blaas (2010), Complexity, accuracy and practical applicability of different biogeochemical model versions, *J. Mar. Syst.*, *81*(1–2), 44–74.
Maeck, A., T. DelSontro, D. F. McGinnis, H. Fischer, S. Flury, M. Schmidt, P. Fietzek, and A. Lorke (2013), Sediment trapping by dams creates methane emission hot spots, *Environ. Sci. Technol.*, *47*(15), 8130–8137.
Maerki, M., B. Muller, C. Dinkel, and B. Wehrli (2009), Mineralization pathways in lake sediments with different oxygen and organic carbon supply, *Limnol. Oceanogr.*, *54*(2), 428–438.
Magnuson, J. J., et al. (2000), Historical trends in lake and river ice cover in the Northern Hemisphere, *Science*, *289*(5485), 1743–1746.
Monteith, D. T., et al. (2007), Dissolved organic carbon trends resulting from changes in atmospheric deposition chemistry, *Nature*, *450*(7169), 537–U539.
Moriasi, D. N., J. G. Arnold, M. W. Van Liew, R. L. Bingner, R. D. Harmel, and T. L. Veith (2007), Model evaluation guidelines for systematic quantification of accuracy in watershed simulations, *Trans. ASABE*, *50*(3), 885–900.
Müller, B., L. D. Bryant, A. Matzinger, and A. Wüest (2012), Hypolimnetic oxygen depletion in eutrophic lakes, *Environ. Sci. Technol.*, *46*(18), 9964–9971.
Paerl, H. W., and V. J. Paul (2012), Climate change: Links to global expansion of harmful cyanobacteria, *Water Res.*, *46*(5), 1349–1363.
Palastanga, V., C. P. Slomp, and C. Heinze (2011), Long-term controls on ocean phosphorus and oxygen in a global biogeochemical model, *Global Biogeochem. Cycles*, *25*, GB3024, doi:10.1029/2010GB003827.
Paraska, D. W., M. R. Hipsey, and S. U. Salmon (2014), Sediment diagenesis models: Review of approaches, challenges and opportunities, *Environ. Modell. Software*, *61*, 297–325.
Peña, M. A., S. Katsev, T. Oguz, and D. Gilbert (2010), Modeling dissolved oxygen dynamics and hypoxia, *Biogeosciences*, *7*(3), 933–957.
Pierson, D. C., et al. (2011), An automated method to monitor lake ice phenology, *Limnol. Oceanogr. Methods*, *9*, 74–83.
Pulkkanen, M., and K. Salonen (2013), Accumulation of low-oxygen water in deep waters of ice-covered lakes cooled below 4°C, *Inland Waters*, *3*, 15–24.
Raike, A., P. Kortelainen, T. Mattsson, and D. N. Thomas (2012), 36 year trends in dissolved organic carbon export from Finnish rivers to the Baltic Sea, *Sci. Total Environ.*, *435*, 188–201.
Read, J. S., L. A. Winslow, G. J. A. Hansen, J. Van Den Hoek, P. C. Hanson, L. C. Bruce, and C. D. Markfort (2014), Simulating 2368 temperate lakes reveals weak coherence in stratification phenology, *Ecol. Modell.*, *291*, 142–150.
Robson, B. J. (2014), State of the art in modelling of phosphorus in aquatic systems: Review, criticisms and commentary, *Environ. Modell. Software*, *61*, 339–359.
Romarheim, A. T., K. Tominaga, G. Riise, and T. Andersen (2015), The importance of year-to-year variation in meteorological and runoff forcing for water quality of a temperate, dimictic lake, *Hydrol. Earth Syst. Sci.*, *19*, 2649–2662.
Rooney, G. G., and F. J. Bornemann (2013), The performance of FLake in the Met Office Unified Model, *Tellus A*, *65*, 21636.
Rucinski, D. K., J. V. DePinto, D. Scavia, and D. Beletsky (2014), Modeling lake Erie's hypoxia response to nutrient loads and physical variability, *J. Great Lakes Res.*, *40*, Supplement 3, 151–161.
Salonen, K., M. Leppäranta, M. Viljanen, and R. D. Gulati (2009), Perspectives in winter limnology: Closing the annual cycle of freezing lakes, *Aquat. Ecol.*, *43*(3), 609–616.
Saloranta, T. M., and T. Andersen (2007), MyLake—A multi-year lake simulation model code suitable for uncertainty and sensitivity analysis simulations, *Ecol. Modell.*, *207*(1), 45–60.
Saloranta, T. M., M. Forsius, M. Jarvinen, and L. Arvola (2009), Impacts of projected climate change on the thermodynamics of a shallow and a deep lake in Finland: Model simulations and Bayesian uncertainty analysis, *Hydrol. Res.*, *40*(2–3), 234–248.
Schwarz, J. I. K., W. Eckert, and R. Conrad (2008), Response of the methanogenic microbial community of a profundal lake sediment (Lake Kinneret, Israel) to algal deposition, *Limnol. Oceanogr.*, *53*(1), 113–121.
Sen, P. K. (1968), Estimates of the regression coefficient based on Kendall's tau, *J. Am. Stat. Assoc.*, *63*(324), 1379–1389.
Skjelkvale, B. L., H. Borg, A. Hindar, and A. Wilander (2007), Large scale patterns of chemical recovery in lakes in Norway and Sweden: Importance of seasalt episodes and changes in dissolved organic carbon, *Appl. Geochem.*, *22*(6), 1174–1180.
Smits, J. G. C., and J. K. L. van Beek (2013), ECO: A generic eutrophication model including comprehensive sediment-water interaction, *Plos ONE*, *8*(7), doi:10.1371/journal.pone.0068104.
Šporka, F., D. Livingstone, E. Stuchlík, J. Turek, and J. Galas (2006), Water temperatures and ice cover in lakes of the Tatra Mountains, *Biologia*, *61*(18), S77–S90.
Staehr, P. A., D. Bade, M. C. Van de Bogert, G. R. Koch, C. Williamson, P. Hanson, J. J. Cole, and T. Kratz (2010), Lake metabolism and the diel oxygen technique: State of the science, *Limnol. Oceanogr. Methods*, *8*, 628–644.
Starrfelt, J., and Ø. Kaste (2014), Bayesian uncertainty assessment of a semi-distributed integrated catchment model of phosphorus transport, *Environ. Sci. Processes Impacts*, *16*, 1578–1587, doi:10.1039/c3em00619k.
Stefan, H. G., and E. B. Preud'homme (1993), Stream temperature estimation from air temperature, *J. Am. Water Resour. Assoc.*, *29*(1), 27–45.
Stefanovic, D. L., and H. G. Stefan (2002), Two-dimensional temperature and dissolved oxygen dynamics in the littoral region of an ice-covered lake, *Cold Reg. Sci. Technol.*, *34*(3), 159–178.
Terzhevik, A. Y., N. I. Pal'shin, S. D. Golosov, R. E. Zdorovennov, G. E. Zdorovennova, A. V. Mitrokhov, M. S. Potakhin, E. A. Shipunova, and I. S. Zverev (2010), Hydrophysical aspects of oxygen regime formation in a shallow ice-covered lake, *Water Resour.*, *37*(5), 662–673.
Trolle, D., D. P. Hamilton, C. A. Pilditch, I. C. Duggan, and E. Jeppesen (2011), Predicting the effects of climate change on trophic status of three morphologically varying lakes: Implications for lake restoration and management, *Environ. Modell. Software*, *26*(4), 354–370.
Trolle, D., J. A. Elliott, W. M. Mooij, J. H. Janse, K. Bolding, D. P. Hamilton, and E. Jeppesen (2014), Advancing projections of phytoplankton responses to climate change through ensemble modelling, *Environ. Modell. Software*, *61*, 371–379.
Vähätalo, A. V., H. Aarnos, and S. Mäntyniemi (2010), Biodegradability continuum and biodegradation kinetics of natural organic matter described by the beta distribution, *Biogeochemistry*, *100*(1–3), 227–240.
Verpoorter, C., T. Kutser, D. A. Seekell, and L. J. Tranvik (2014), A global inventory of lakes based on high-resolution satellite imagery, *Geophys. Res. Lett.*, *41*, 6396–6402, doi:10.1002/2014GL060641.
von Wachenfeldt, E., and L. J. Tranvik (2008), Sedimentation in boreal lakes—The role of flocculation of allochthonous dissolved organic matter in the water column, *Ecosystems*, *11*(5), 803–814.
von Wachenfeldt, E., S. Sobek, D. Bastviken, and L. J. Tranvik (2008), Linking allochthonous dissolved organic matter and boreal lake sediment carbon sequestration: The role of light-mediated flocculation, *Limnol. Oceanogr.*, *53*(6), 2416–2426.

Vrugt, J. A., C. J. F. ter Braak, C. G. H. Diks, B. A. Robinson, J. M. Hyman, and D. Higdon (2009), Accelerating Markov chain Monte Carlo simulation by differential evolution with self-adaptive randomized subspace sampling, *Int. J. Nonlinear Sci. Numer. Simul.*, *10*(3), 273–290.

Vuorenmaa, J., K. Salonen, L. Arvola, J. Mannio, M. Rask, and P. Horppila (2014), Water quality of a small headwater lake reflects long-term variations in deposition, climate and in-lake processes, *Boreal Environ. Res.*, *19*, 47–65.

Wetzel, R. G. (2001), *Limnology: Lake and River Ecosystems*, 3rd ed., Academic Press, San Diego.

Weyhenmeyer, G. A., D. M. Livingstone, M. Meili, O. Jensen, B. Benson, and J. J. Magnuson (2011), Large geographical differences in the sensitivity of ice-covered lakes and rivers in the Northern Hemisphere to temperature changes, *Global Change Biol.*, *17*(1), 268–275.

White, D. M., H. M. Clilverd, A. C. Tidwell, L. Little, M. R. Lilly, M. Chambers, and D. Reichardt (2008), A tool for modeling the winter oxygen depletion rate in Arctic lakes, *J. Am. Water Resour. Assoc.*, *44*(2), 293–304.

Wilson, D., H. Hisdal, and D. Lawrence (2010), Has streamflow changed in the Nordic countries?—Recent trends and comparisons to hydrological projections, *J. Hydrol.*, *394*(3–4), 334–346.

Zveryaev, I. I., and S. K. Gulev (2009), Seasonality in secular changes and interannual variability of European air temperature during the twentieth century, *J. Geophys. Res.*, *114*, D02110, doi:10.1029/2008JD010624.